Developmental Cell, Vol. 6, 483–495, April, 2004, Copyright ©2004 by Cell Press

Cell Shape, Cytoskeletal Tension, and RhoA Regulate Stem Cell Lineage Commitment

Rowena McBeath,[1] Dana M. Pirone,[2] Celeste M. Nelson,[2] Kiran Bhadriraju,[2] and Christopher S. Chen[1,2,3,*]
[1]The Cellular and Molecular Medicine Program
[2]Department of Biomedical Engineering
[3]Department of Oncology
The Johns Hopkins University School of Medicine
Baltimore, Maryland 21205

Summary

Commitment of stem cells to different lineages is regulated by many cues in the local tissue microenvironment. Here we demonstrate that cell shape regulates commitment of human mesenchymal stem cells (hMSCs) to adipocyte or osteoblast fate. hMSCs allowed to adhere, flatten, and spread underwent osteogenesis, while unspread, round cells became adipocytes. Cell shape regulated the switch in lineage commitment by modulating endogenous RhoA activity. Expressing dominant-negative RhoA committed hMSCs to become adipocytes, while constitutively active RhoA caused osteogenesis. However, the RhoA-mediated adipogenesis or osteogenesis was conditional on a round or spread shape, respectively, while constitutive activation of the RhoA effector, ROCK, induced osteogenesis independent of cell shape. This RhoA-ROCK commitment signal required actin-myosin-generated tension. These studies demonstrate that mechanical cues experienced in developmental and adult contexts, embodied by cell shape, cytoskeletal tension, and RhoA signaling, are integral to the commitment of stem cell fate.

Introduction

Connective tissue cells differ greatly in phenotype. Although they descend from a common mesenchymal stem cell (MSC) precursor, differentiated adipocytes are round and fat-laden (Green and Kehinde, 1974; Gregoire et al., 1998), while osteoblasts vary from elongated to cuboidal, depending on their matrix deposition activity (Grigoriadis et al., 1988; Sikavitsas et al., 2001). The shapes of these cells serve their specialized functions, while simultaneously driving their multicellular organization (Thompson, 1992). A round, spherical shape allows for maximal lipid storage in adipose tissue, while cell spreading facilitates osteoblast matrix deposition during bone remodeling (Parfitt, 1984). These different cell morphologies are thought to arise from changes in the expression of integrins, cadherins, and cytoskeletal proteins (Gumbiner, 1996) during stem cell commitment, the process by which a cell chooses its fate, and differentiation, the subsequent development of lineage-specific characteristics (Hu et al., 1995).

While differentiation may cause changes in cell shape, several studies have noted that changes in cell shape themselves can alter the differentiation of precommitted mesenchymal lineages. Spiegelman and Ginty (1983) found that when the adipogenic cell line 3T3-F442A was allowed to attach and spread on surfaces coated with fibronectin, differentiation as evidenced by lipogenic gene expression was inhibited. These inhibitory effects of cell spreading on adipogenic differentiation were reversed when cells were kept round, or upon disruption of the actin cytoskeleton (Spiegelman and Ginty, 1983; Rodriguez Fernandez and Ben-Ze'ev, 1989). In contrast, cell spreading has been shown to increase osteoblast differentiation in preosteoblastic progenitors as measured by increased osteopontin and osteocalcin expression (Carvalho et al., 1998; Thomas et al., 2002). In this case, differentiation requires an intact cytoskeleton (Pavalko et al., 1998; Toma et al., 1997). While changes in cell shape and cytoskeletal integrity appear to be important in differentiation of certain lineages, little is known about whether cell shape affects earlier developmental stages, such as the commitment of a multipotential stem cell.

Recently, human mesenchymal stem cells (hMSCs) have been isolated from adult bone marrow that are capable of differentiation to multiple lineages important to connective tissue (Pittenger et al., 1999). These adherent cells differentiate into adipocytes, osteoblasts, and chondrocytes when exposed to various growth factor combinations (Pittenger et al., 1999, 2002). Importantly, it was noted that differentiation into these lineages only occurred if cells were plated at appropriate densities. While much is known about how each of the growth factors regulates lineage specification and differentiation, little is known about the significance of the cell density requirement in these protocols. We hypothesized that these differences in cell density confer differences in cell shape and that cell shape acts as a cue in the commitment process.

While cell shape has been shown to regulate biological processes such as proliferation (Chen et al., 1997) and differentiation (Watt et al., 1988; Roskelley et al., 1994), the molecular basis of these cell shape-mediated effects has remained ill defined. Recent studies suggest that cell shape may affect activity in Rho family GTPases (Ren et al., 1999). Numerous studies show that Rho GTPases are critical to proliferation (Hill et al., 1995; Welsh et al., 2001) and differentiation (Takano et al., 1998; Sordella et al., 2003). Recently, a cytoskeletal-independent role for Rho was proposed to determine the differentiation of mouse embryonic fibroblasts into adipocytes and myoblasts (Sordella et al., 2003), suggesting a role for Rho GTPase signaling in early cellular developmental processes.

Here, we set out to examine whether changes in cell shape can regulate commitment of mesenchymal cells to different lineages, and if so, how. We chose to use hMSCs to examine the commitment process, as the ability of these cells to become adipocytes and osteoblasts from multipotent mesenchymal precursor cells has been well documented (Friedenstein, 1976; Caplan,

*Correspondence: cchen@bme.jhu.edu

1991; Pittenger et al., 1999). Using a micropatterning technique to control cell shape and degree of cell spreading with single-cell precision, thousands of cells at a time, we have identified cell shape as a key regulator in hMSC commitment to the osteoblast or adipocyte lineages. This shape-dependent control of lineage commitment is mediated by RhoA activity, specifically via its effects on ROCK-mediated cytoskeletal tension. In fact, controlling RhoA activity completely supplanted the need for soluble differentiation factors. This study demonstrates that cell shape and cytoskeletal mechanics drive stem cell commitment, and it points to a molecular pathway by which this occurs.

Results

hMSC Commitment Depends on Cell Density

Previous studies suggested that initial plating densities affect optimal differentiation of hMSCs (Pittenger et al., 1999). To confirm this effect, we examined hMSC differentiation to the osteoblastic and adipogenic lineages when plated at different densities in osteogenic or adipogenic culture media. Early passage hMSCs were plated at four densities (1000 to 25,000 cells/cm^2) and cultured in osteogenic or adipogenic differentiation media for up to 4 weeks. Cells were collected every week and stained for alkaline phosphatase or lipids, markers of osteogenesis and adipogenesis, respectively. At the lowest plating density, cells attached with little interaction between neighboring cells. At the highest density, cells were effectively confluent upon plating. In adipogenic media, cells seeded at low density did not form the stereotypic fat globules indicative of adipogenesis, but did at high density (Figures 1A and 1C). Conversely, in osteogenic media, more cells expressed alkaline phosphatase at low density than at high density (Figures 1B and 1D). As cells generally stained intensely for the markers or not at all, the degree of adipogenesis or osteogenesis was quantified by counting the percentage of cells labeled (Figures 1E and 1F; Supplemental Figure S1 [http://www.developmentalcell.com/cgi/content/full/6/4/483/DC1]). To confirm these findings, we performed semiquantitative RT-PCR on 1-week cultures to detect molecular markers of the adipocyte and osteoblast lineages. Adipocyte markers lipoprotein lipase (Lpl) and peroxisome proliferator activator receptor γ 2 (PPARγ2), and osteoblast markers alkaline phosphatase (AP) and core binding factor α 1 (Cbfa1), confirmed the density-dependent effects on hMSC differentiation (Figures 1I and 1J).

One uncontrolled and confounding aspect of these extended experiments was cell proliferation. Because cells continued to divide during the course of the study, cell density increased with time, and increased at different rates depending on experimental conditions (Figures 1G and 1H). Furthermore, proliferation rates increased at low plating densities and in osteogenic differentiation media, and arrested at high densities and in adipogenic differentiation media. These observations raised the possibility that proliferation or the cell cycle itself may be linked to lineage commitment, as has been suggested by other studies (Shao and Lazar, 1997; Fajas, 2003).

To eliminate these ambiguities, we examined differentiation in proliferation-arrested cells. We administered increasing concentrations of a DNA polymerase inhibitor (aphidicolin) or an alkylating agent (mitomycin C) to hMSCs to identify working concentrations of inhibitors. Prolonged exposure to aphidicolin (2 μg/ml) or mitomycin C (10 μg/ml) demonstrated growth arrest without obvious toxicity (Figure 2A). Aphidicolin or mitomycin C-treated hMSCs were plated at high or low density in adipogenic or osteogenic media and stained for lipids or AP after 1 week. Irrespective of cell proliferation, hMSCs became adipocytes only at high plating density, while osteoblastic commitment was favored at low density (Figures 2B and 2C). Thus, the density effects on both adipocyte and osteoblast differentiation occur independently of cell proliferation.

To more directly investigate the role of cell density in commitment, we examined adipogenesis and osteogenesis simultaneously in cultures exposed to a mixed media containing both adipogenic and osteogenic factors, as well as the proliferation inhibitors aphidicolin or mitomycin C. Cells were plated at high or low densities for 4 weeks and costained for AP and lipids (Figure 2D). At high densities, cells favored adipogenesis, while cells switched to an osteogenic fate at low densities (Figures 2E and 2F).

While these findings suggested that plating density might directly affect hMSC lineage commitment, a possible mechanism for the enrichment of specific lineages is through a density-dependent, differential survival advantage for adipocytes versus osteoblasts. To explore this possibility, we investigated whether hMSCs that had already differentiated into adipocytes or osteoblasts exhibited preferential survival in low- or high-density culture. hMSCs were differentiated into adipocytes at high plating density or into osteoblasts at low plating density, and replated at low or high density, respectively. After 1 week, adipocytes and osteoblasts showed equally high viability, irrespective of replating density (Figure 2G). These results suggest that initial plating density does not affect the lineage outcomes by selecting adipogenic subpopulations at high density, or osteogenic subpopulations at low density. Instead, cell density appeared to directly alter whether hMSCs differentiated into one lineage versus another.

hMSC adipogenesis and osteogenesis are both thought to involve distinct commitment and differentiation steps (Smas and Sul, 1997; Gregoire et al., 1998; Franceschi, 1999). To investigate whether cell density can act specifically on the lineage commitment process, prior to differentiation, hMSCs were plated at high or low density for 4 days without soluble differentiation factors. Cells were then suspended and replated at high or low density for 1 week in mixed differentiation media conditions. As in the earlier experiments, high replating density induced adipogenesis while suppressing osteogenesis. Interestingly, preculturing hMSCs at low density significantly inhibited adipogenic commitment (Figure 2H), while preculturing at high density prevented osteogenesis (Figure 2I). These findings suggest that hMSC lineage commitment can be initiated independently from the downstream steps of differentiation, and that initial plating density alone can drive this commitment.

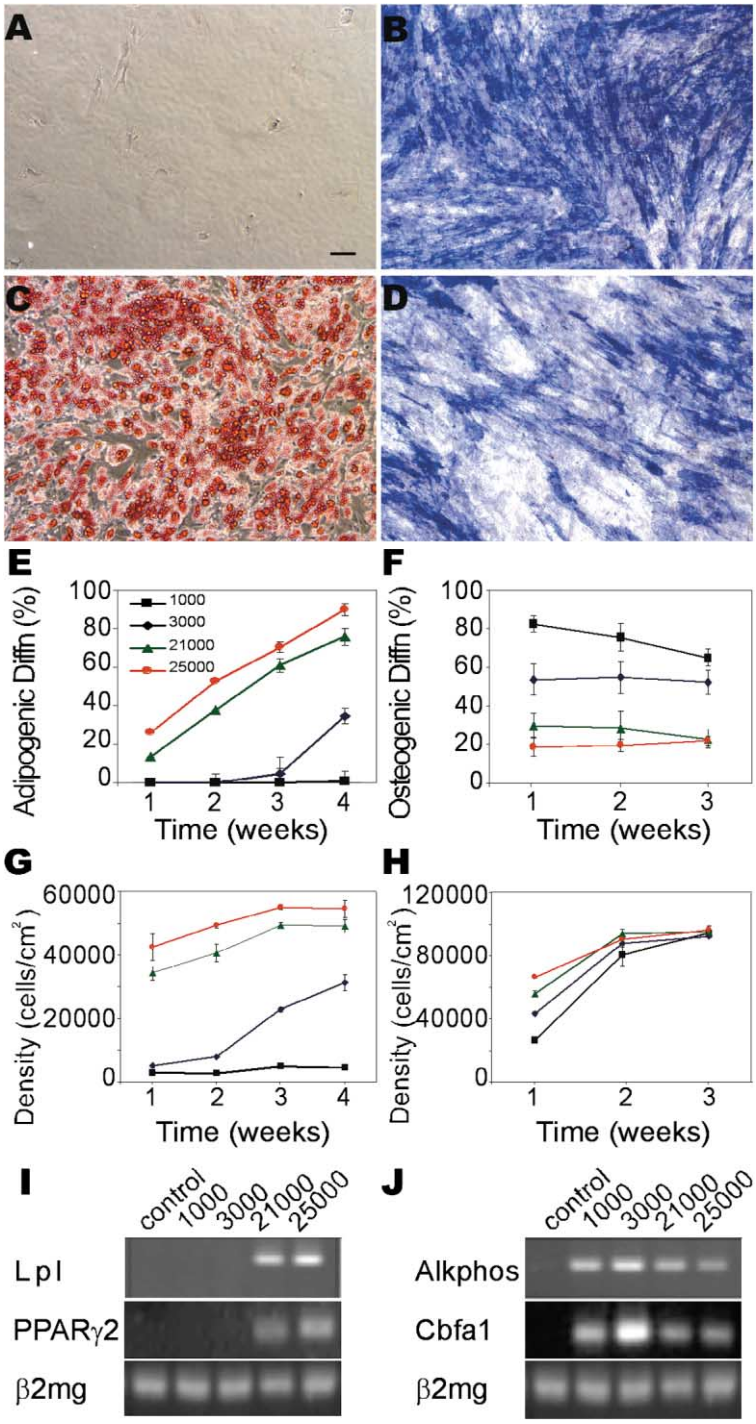

Figure 1. hMSC Adipogenesis versus Osteogenesis Depends on Cell Density

(A–D) Brightfield images of hMSCs plated at 1000 cells/cm^2 (A and B) or 25,000 cells/cm^2 (C and D), cultured for 4 weeks in adipogenic (A and C) or 3 weeks in osteogenic (B and D) differentiation media, and stained for the presence of lipids (A and C) or alkaline phosphatase (B and D). Scale bar = 200 μm.

(E and F) Plot of hMSC percentage differentiation over time when cultured at 1000, 3000, 21,000, or 25,000 cells/cm^2 in the presence of adipogenic differentiation media (E) or osteogenic differentiation media (F).

(G and H) Plot of hMSC relative density over time when plated at the different seeding densities in the presence of adipogenic (G) or osteogenic (H) differentiation media.

(I and J) RT-PCR for adipogenic (I) or osteogenic (J) differentiation markers of hMSCs plated at the indicated densities and cultured in adipogenic (I) or osteogenic (J) differentiation media. Samples were collected after 1 week in culture. Control, cells plated at 3000 cells/cm^2 exposed to nondifferentiating growth media; Lpl, lipoprotein lipase; PPARγ2, peroxisome proliferator activated receptor γ 2; Alkphos, alkaline phosphatase; Cbfa1, core binding factor α 1; β2mg, β-2-microglobulin.

Cell Shape Drives hMSC Commitment

Many cues in the local environment change when cells are grown at different densities. With increasing density, cell adhesion and spreading against the substrate decrease, while cell-cell contact and paracrine signaling increase. Conventional techniques are unable to separate the effects of these different cues (Nelson and Chen, 2002). Here, using micropatterned substrates to control the degree of cell spreading against the substrate in the absence of cell-cell communication, we explored specifically the role of cell shape on stem cell commitment. We microcontact printed fibronectin onto polydimethylsiloxane (PDMS) substrates to generate "islands" of fibronectin surrounded by regions blocked with the nonadhesive, Pluronic F108. hMSCs plated onto these islands attached as single cells per island, and spread to different degrees depending on the size of the islands (1024 or 10,000 μm^2; Figure 3A). The cells were cultured on these islands in mixed media for 1 week, then fixed and stained for both AP and lipids.

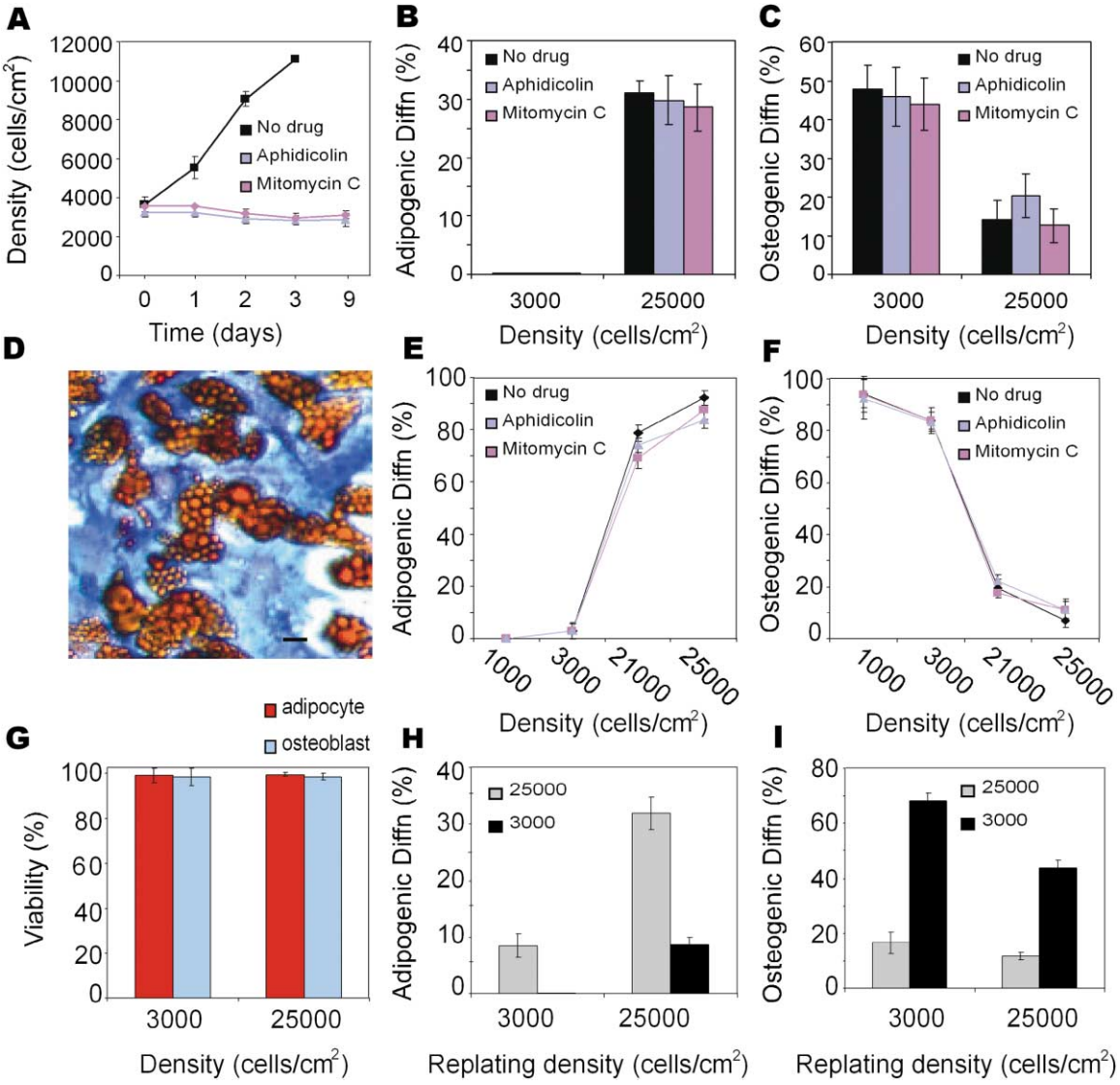

Figure 2. Density-Dependent Adipogenesis versus Osteogenesis Results from Differential Lineage Commitment, Not Differential Proliferation or Survival

(A) Plot of hMSC density over time with or without aphidicolin (2 μg/ml) or mitomycin C (10 μg/ml) treatment.

(B and C) Percentage of hMSC adipogenesis (B) or osteogenesis (C) at 3000 or 25,000 cells/cm^2 plating density after 1 week with or without aphidicolin or mitomycin C treatment.

(D) Brightfield image of hMSCs exposed to mixed media (combined osteogenic and adipogenic media). Alkaline phosphatase stains blue; lipids stain red. Scale bar = 50 μm.

(E and F) Percentage of hMSC adipogenic (E) or osteogenic (F) differentiation 4 weeks after plating at 1000, 3000, 21,000, or 25,000 cells/cm^2 in mixed media conditions with or without aphidicolin or mitomycin C treatment.

(G) Percentage of adipocyte or osteoblast viability when replated at 3000 or 25,000 cells/cm^2, respectively.

(H and I) Percentage of adipogenesis (H) or osteogenesis (I) when hMSCs initially plated at high (25,000 cells/cm^2) or low density (3000 cells/cm^2) in nondifferentiating growth media were replated at low or high density and cultured for 1 week in mixed media.

hMSC adipogenesis occurred only on small islands, osteogenesis occurred only on large islands, and a mixture of both lineages was found on intermediate-sized islands (Figure 3B). The percentage of lipid- or AP-stained cells was determined for islands containing single cells, demonstrating a marked effect of cell shape on commitment. Similar results were obtained when inhibiting proliferation by patterning the cells in the presence of aphidicolin (Figure 3C). To address whether the lineage enrichment on micropatterns resulted from differential apoptotic selection of adipocytes versus osteoblasts, cells were plated onto small or large islands, counted, and cultured in mixed media with aphidicolin for 1 week. Cells were then recounted and assayed for viability. Micropatterning did not cause significant decreases in total cell number or viability (Figure 3D), indicating that the highly enriched lineage-specific cell populations are not selected based on preferential survival

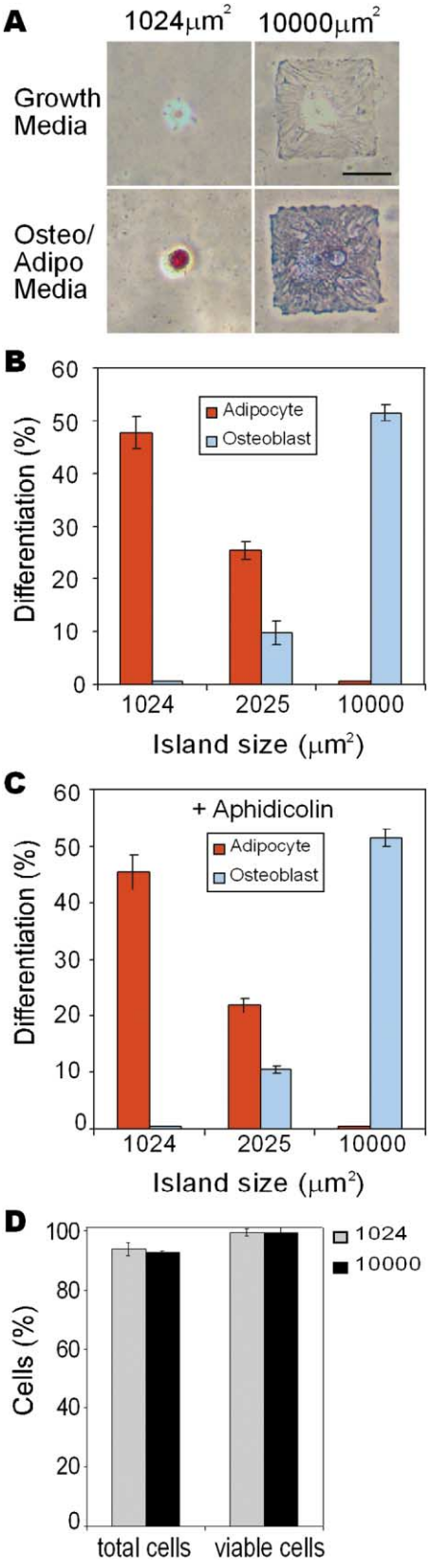

Figure 3. Cell Shape Drives hMSC Commitment

(A) Brightfield images of hMSCs plated onto small (1024 μm^2) or large (10,000 μm^2) fibronectin islands after 1 week in growth or mixed media. Lipids stain red; alkaline phosphatase stains blue. Scale bar = 50 μm.

(B and C) Percentage differentiation of hMSCs plated onto 1024, 2025, or 10,000 μm^2 islands after 1 week of culture in mixed media without (B) or with (C) aphidicolin (2 μg/ml) treatment.

(D) Percentage of hMSCs remaining and viable after 1 week of culture on 1024 or 10,000 μm^2 islands in mixed media and aphidicolin treatment.

on the micropatterns. In all, these results suggest that changes in cell shape alone are sufficient to mediate the switch in hMSC commitment between adipogenic and osteogenic fates. Furthermore, because the effects of cell shape on commitment persist in the absence of proliferation or apoptosis, the effects of cell shape on proliferation or survival are distinct from those on cell fate determination.

hMSC Commitment Varies with Changes in Cytoskeletal Tension

Changes in cell shape may be transduced into a regulatory signal by several structures in the cell, including the actin cytoskeleton itself (Huang et al., 1998). In fact, sparsely plated and well-spread hMSCs exhibited more prominent stress fibers as compared to densely plated and unspread cells. To examine whether the actin cytoskeleton was involved in the shape-mediated commitment process, hMSCs were first cultured with the actin-disrupting agent cytochalasin D in mixed differentiation media conditions at low plating density. Lipid and AP staining revealed that disrupting actin increased adipogenesis and decreased osteogenesis as compared to untreated controls (Figures 4A and 4B). While these data suggested that the actin cytoskeleton might be important in the commitment process, we observed that the drug treatment also caused cells to become rounded (Figure 4A). Thus it remained unclear whether cytochalasin D affected commitment primarily by changing cell shape or disrupting the actin cytoskeleton.

To address this ambiguity, we impaired the actin cytoskeleton by specifically inhibiting myosin-generated cytoskeletal tension. hMSCs were cultured in mixed media in the presence of Y-27632 (10 μM), an inhibitor of Rho kinase (ROCK), the Rho effector involved in myosin activation (Kimura et al., 1996). In the presence of Y-27632, cells remained spread and morphologically similar to untreated controls (Figure 4A). Much like cytochalasin D-treated cells, ROCK-inhibited cells exhibited decreased AP and increased lipid production as compared to untreated controls (Figure 4B). While this shift in lineages suggests that cell shape-mediated commitment involves actomyosin contractility, it is possible that drug treatment selects preadipogenic hMSCs by causing preosteogenic cells to die. To exclude this possibility, cells were first differentiated to adipocytes or osteoblasts, counted, then treated with cytochalasin D or Y-27632 for 1 week. Cells were then recounted and assayed to determine total cell number and viability. Treatment with cytochalasin D or Y-27632 did not significantly alter total number or viability of differentiated adipocytes or osteoblasts (Figure 4C). These findings suggest a role for the actomyosin cytoskeleton in hMSC commitment.

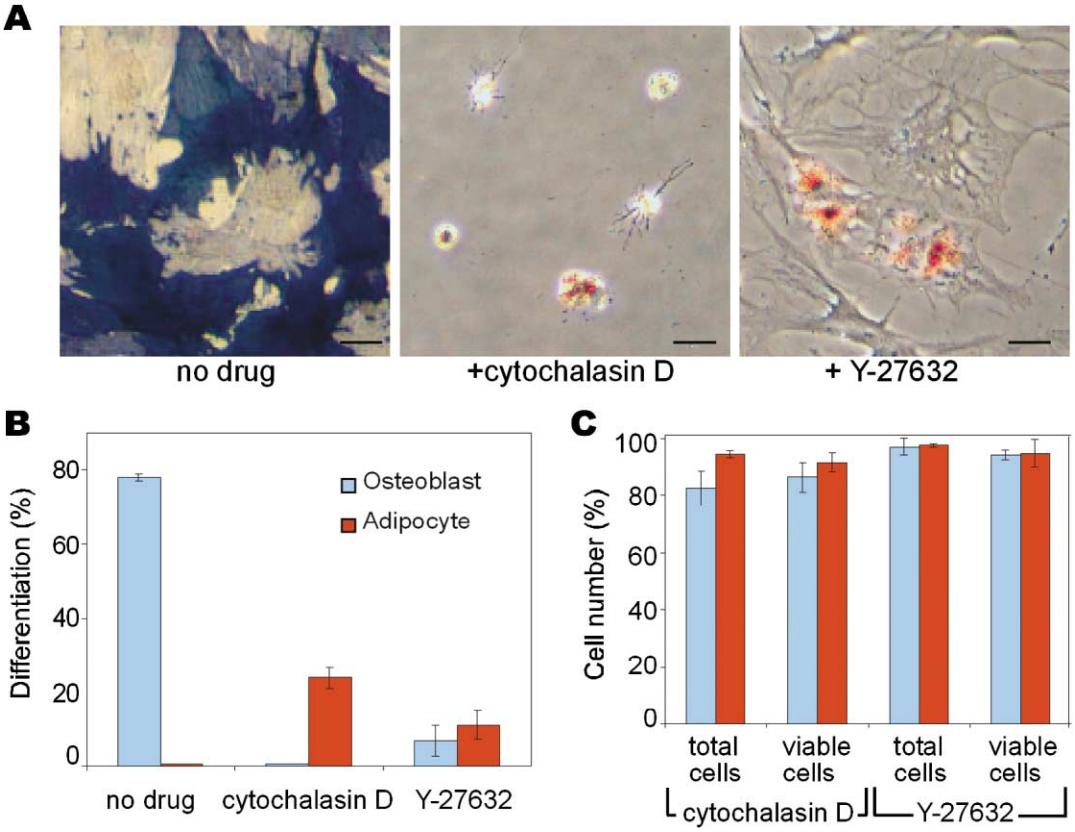

Figure 4. hMSC Commitment Varies with Changes in Cytoskeletal Tension

(A and B) Brightfield image (A) and percentage differentiation (B) of hMSCs plated at low density (3000 cells/cm^2) in mixed media after 1 week without or with cytochalasin D (1 μg/ml) or Y-27632 (10 μM) treatment.

(C) Percentage of remaining and viable osteoblasts or adipocytes after 1 week of cytochalasin D (1 μg/ml) or Y-27632 (10 μM) treatment.

hMSC Shape Regulates RhoA Activity

The dependence of the adipogenic-to-osteogenic shift on cell spreading and ROCK-mediated cytoskeletal tension raised the possibility that contractile activity increases with cell spreading. As the RhoA GTPase is a central regulator of contractility in many cells (Chrzanowska-Wodnicka and Burridge, 1996; Etienne-Manneville and Hall, 2002), we investigated whether RhoA activity might transduce shape into a regulatory signal. To examine the levels of active RhoA under various differentiation conditions, cells were plated at low (4000 cells/cm^2) or high (12,000 cells/cm^2) densities and cultured in osteogenic, adipogenic, or growth media (Figure 5A). Cells were harvested at days 2, 4, and 6. At the time of harvest, cells plated at low densities were more well-spread (Figure 5B) and showed more pronounced stress fiber formation than those plated at high densities.

We first confirmed that serum stimulation of starved hMSCs could activate RhoA, as has been shown for many other cell types (Ren et al., 1999). Confluent hMSCs were serum starved, exposed to growth media, and lysed. GTP-bound RhoA was isolated using the Rho binding domain of rhotekin as described by Ren et al. (2000). Active and total RhoA were normalized to total protein and blotted. Minutes after serum stimulation, RhoA activity increased dramatically (Figure 5C). We then examined the levels of active, GTP-bound RhoA under osteogenic and adipogenic plating conditions. On all days, RhoA activity was significantly higher in low- versus high-density culture, regardless of culture media (Figure 5D). Furthermore, osteogenic media further enhanced RhoA activity, while adipogenic media suppressed activation, though to a lesser extent. Thus, RhoA activity is greatest when cells are subconfluent in osteogenic media, and lowest when cells are confluent in adipogenic media, spanning nearly a 7-fold difference (Figure 5D). These findings suggest the possibility that RhoA may be involved in the final common pathway that transduces cell density and soluble factors to regulate hMSC commitment.

To examine whether the increased RhoA signaling at subconfluence was specifically due to increased cell spreading, we patterned hMSCs onto small or large islands and, on day 3, measured kinase activity of the downstream Rho effector, ROCK. ROCK activity in spread cells was significantly greater than that on round cells; this activity was abrogated by treatment with Y-27632 (Figure 5E). Together, these findings demonstrate that cell shape directly affects RhoA and ROCK activity.

RhoA Regulates the hMSC Commitment Switch between Osteogenic or Adipogenic Fate

As high levels of active RhoA correlated to osteogenic conditions and low levels to adipogenic conditions, we

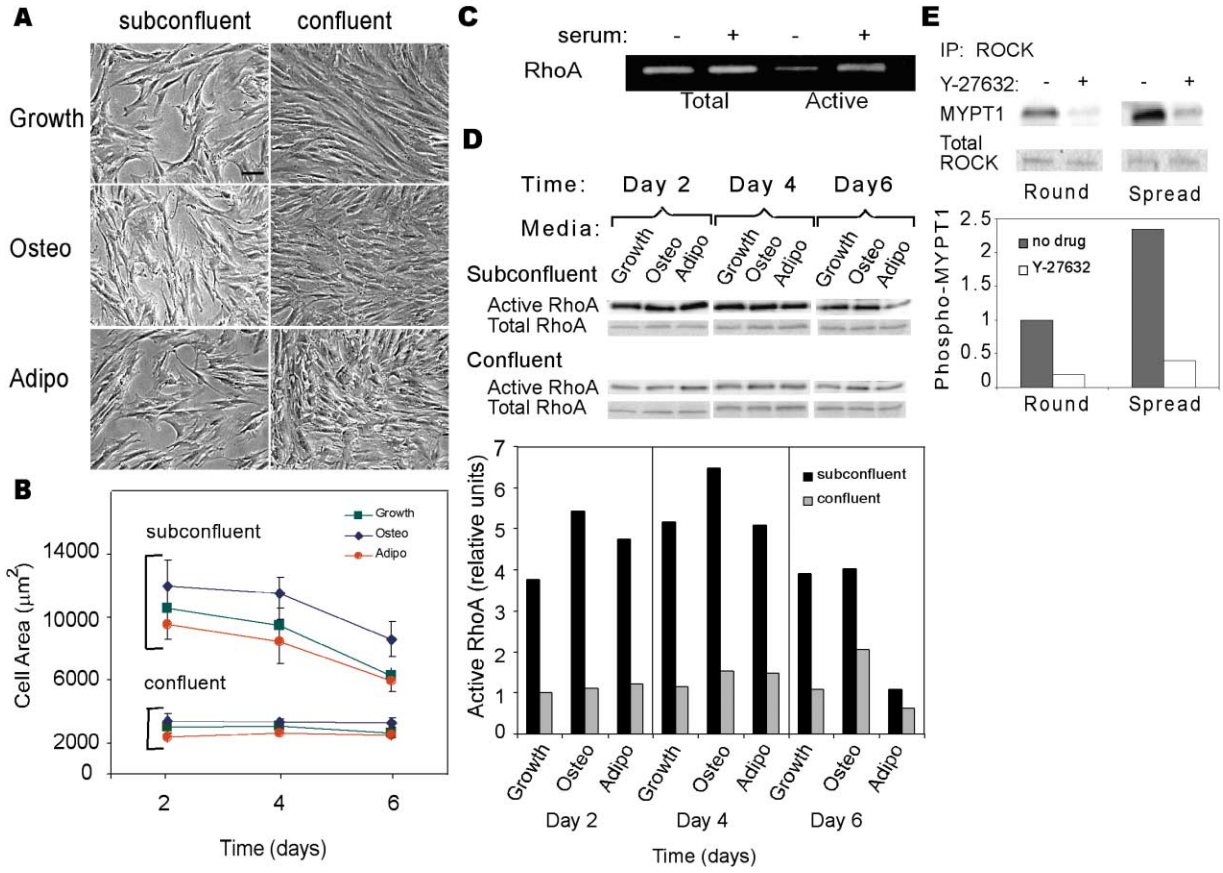

Figure 5. hMSC Shape Regulates RhoA Activity

(A) Phase contrast images of hMSCs in growth medium (Growth), osteogenic (Osteo), or adipogenic differentiation media (Adipo), 2 days after plating at 4000 or 12,000 cells/cm^2. Scale bar = 100 μm.

(B) Morphometric analysis of area of cell spreading at days 2, 4, and 6 after plating at subconfluent (sc) or confluent (c) density.

(C) Western blot of total and active RhoA in serum-starved hMSCs, with (+) or without (−) serum stimulation.

(D) Western blots and quantification of active RhoA in hMSCs in growth and differentiation conditions, on days 2, 4, and 6 after plating at subconfluent or confluent density.

(E) Western blots and quantification of MYPT1 phosphorylation by ROCK kinase immunoprecipitated from round or spread cells at day 3 of culture, with or without the ROCK inhibitor Y-27632.

chose to investigate whether RhoA activity itself could directly regulate hMSC lineage commitment. We used adenoviral constructs of constitutively active (RhoA-V14) or dominant-negative (RhoA-N19) RhoA in tandem with GFP to directly manipulate RhoA. hMSCs in nondifferentiating (growth) media conditions were infected with RhoA-V14, RhoA-N19, or GFP control virus, then fixed and stained for AP and lipids after 1 week. In growth media, GFP-infected and uninfected cells did not exhibit osteogenesis or adipogenesis. Remarkably, hMSCs infected with constitutively active RhoA-V14 became osteoblasts while those infected with dominant-negative RhoA-N19 became adipocytes in the absence of any inducing factors, as measured by AP or lipid production as well as by RT-PCR for lineage markers (Figures 6A–6C). The degree of commitment caused by RhoA viral infection was comparable to that from standard induction protocols (Figure 6D).

These results show that increasing or decreasing RhoA activity alone can switch hMSC commitment to osteoblasts or adipocytes even in nondifferentiating media. To investigate whether RhoA is necessary for hMSC lineage commitment, we examined whether cells at an intermediate density (12,000 cells/cm^2) exposed to adipogenic conditions would differentiate when infected with RhoA-V14, while osteogenesis was examined in RhoA-N19-infected hMSCs exposed to osteogenic media. Under adipogenic conditions, adipogenesis was inhibited by constitutively active RhoA. Remarkably, these RhoA-V14-infected cells underwent significant osteogenesis. Similarly, dominant-negative RhoA abrogated osteogenic media-induced osteogenesis, and redirected cells to the adipogenic differentiation program (Figure 6E). These studies suggest that RhoA can fully replace the signals mediated by the soluble differentiation factors.

RhoA Regulates hMSC Commitment through ROCK and Cytoskeletal Integrity

RhoA has many effectors; some act on cytoskeletal structure and mechanics, while others do not. To examine whether RhoA-dependent commitment depends on its cytoskeletal effects, RhoA-V14-infected hMSCs were

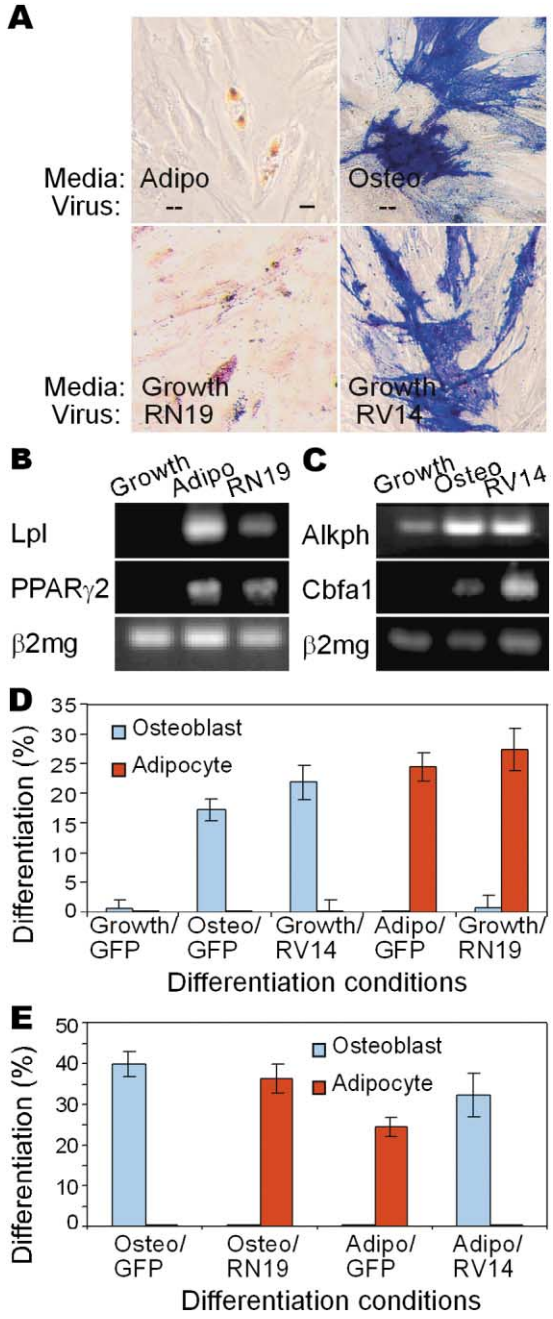

Figure 6. RhoA Regulates the hMSC Commitment Switch between Osteogenic or Adipogenic Fate

(A) Brightfield images of hMSCs after 1 week in differentiation media or virus infection. Adipo, adipogenic media; Osteo, osteogenic media; Growth, growth media; RN19, transduction of dominant-negative RhoA-N19; RV14, transduction of constitutively active RhoA-V14. Lipids stain red; alkaline phosphatase stains blue. Scale bar = 50 μm.

(B and C) RT-PCR of adipogenic (B) and osteogenic (C) lineage markers of hMSCs harvested after 1 week in growth or differentiation media, RhoA-N19 or RhoA-V14 virus infection.

(D and E) Percentage adipogenic or osteogenic differentiation of hMSCs after 1 week in indicated media and viral transduction (media/viral) condition.

treated with cytochalasin D (1 μg/ml) during the differentiation process. The osteogenic shift induced by constitutively active RhoA-V14 was abrogated by disrupting actin (Figure 7A). Treatment with the ROCK inhibitor Y-27632 (10 μM) or the myosin II inhibitor blebbistatin (50 μM) also abrogated RhoA-V14-induced osteogenesis.

Interestingly, the redirecting of hMSC commitment by manipulating RhoA signaling coincided with changes in cell shape. That is, osteogenesis was associated with spread cells, while adipogenesis led to cell rounding. To directly examine whether RhoA fully mediates the commitment signals affected by cell shape as well as those from soluble factors, we examined whether activating RhoA rescues osteogenesis in round cells and inactivating RhoA rescues adipogenesis in spread cells. hMSCs were plated onto small and large fibronectin islands and infected with RhoA-N19 or RhoA-V14. Round cells infected with RhoA-N19 became adipocytes, while spread cells infected with RhoA-V14 became osteoblasts (Figures 7B and 7C). The osteogenesis induced in these cells was blocked by both Y-27632 and blebbistatin (Figure 7D), indicating that the tension generating system is required in this process. Surprisingly, constitutively active RhoA-V14-infected cells failed to form osteoblasts when round, and cell spreading blocked dominant-negative RhoA-N19-induced adipogenesis (Figures 7B and 7C). That is, cell shape and RhoA activity are both necessary, but neither is sufficient, to drive the switch in hMSC commitment.

While RhoA did not appear to be downstream of the cell spreading requirement for osteogenesis, we explored whether ROCK fully mediated the osteogenic commitment signal in both round and spread cells. hMSCs were plated onto small and large fibronectin islands and infected with adenovirus containing constitutively active ROCK (ROCKΔ3). Both round and spread cells infected with ROCKΔ3 became osteoblasts, and the ROCKΔ3-induced osteogenesis was inhibited by blebbistatin (Figure 7E). Together, these findings suggest that, while RhoA is downstream of soluble differentiation signals, cell shape-mediated control of the adipogenic-to-osteogenic commitment switch is regulated via ROCK-induced cytoskeletal tension.

Discussion

Like many stem cells, hMSCs differentiate into distinct lineages depending on what local cues are present in their environment. Among the many cues required for lineage-specific differentiation of hMSCs in vitro, initial cell plating density appeared to be critically important but poorly understood (Pittenger et al., 1999). We now show that plating density alters cell shape, which provides the critical cue that regulates an adipogenic-osteogenic switch in hMSC lineage commitment. Furthermore, we demonstrate that this commitment switch is mediated through the RhoA-ROCK signaling pathway.

Previous studies have suggested that changes in cell shape can regulate the degree of development of lineage-specific markers, or differentiation, in precommitted preadipocytes or preosteoblasts (Spiegelman and Ginty, 1983; Thomas et al., 2002). It has been shown that RhoA also can promote differentiation in precommitted

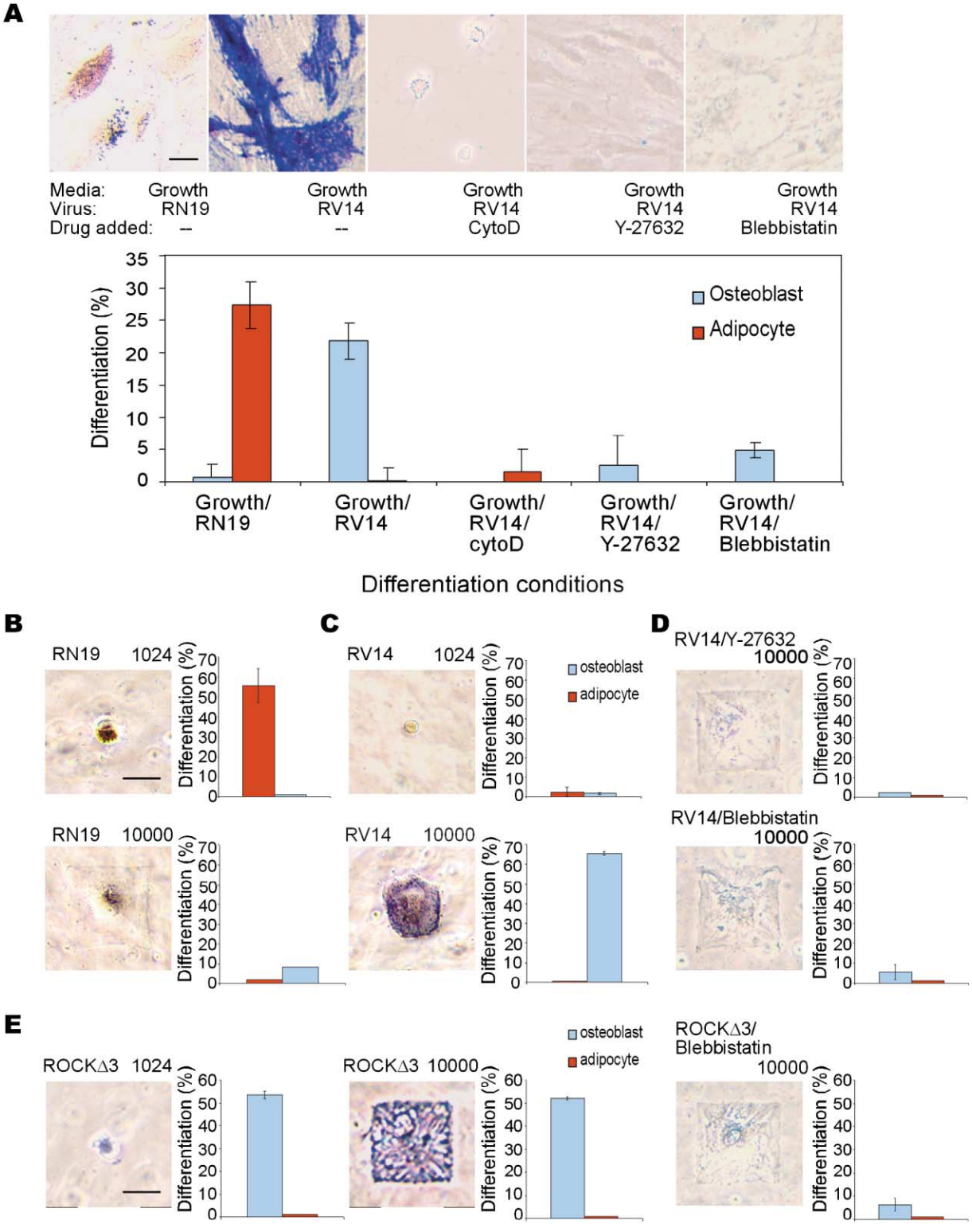

Figure 7. RhoA Effects on hMSC Commitment Require Cytoskeletal Integrity and ROCK Activity

(A) Brightfield images (top panels) of hMSCs infected with RhoA-N19 (RN19) or RhoA-V14 (RV14) in growth media conditions alone with or without cytochalasin D (1 μg/ml), Y-27632 (10 μM), or blebbistatin (50 μM) treatment for 1 week. Scale bar = 50 μm. Percentage (lower panel) of hMSC adipogenic or osteogenic differentiation.

(B–D) Brightfield images and bar graphs of hMSC percent differentiation when plated onto 1024 or 10,000 μm^2 islands and transduced with dominant-negative RhoA-N19 (B), constitutively active RhoA-V14 (C), or constitutively active RhoA-V14 with 10 μM Y-27632 or 50 μM blebbistatin (D) treatment for 1 week. Scale bar = 50 μm.

(E) Brightfield images of hMSCs plated onto 1024 or 10,000 μm^2 islands and transduced with constitutively active ROCK (ROCKΔ3), or transduced with constitutively active ROCK and treated with 50 μM blebbistatin for 1 week. Scale bar = 50 μm.

smooth and skeletal muscle systems (Carnac et al., 1998; Takano et al., 1998; Wei et al., 1998; Charrasse et al., 2002). Sordella et al. (2003), having noted decreased adipogenesis and increased myogenesis of embryonic fibroblasts derived from mice deficient in an inactivator of Rho, p190-B RhoGAP, suggested the possibility that RhoA may affect lineage commitment as well as differentiation, though provided no direct evidence for this linkage. The demonstration that a clonal population of hMSCs can become adipocytes or osteoblasts without altering proliferation or apoptosis now provides direct evidence that these shape- and RhoA-mediated signals can act at an earlier stage in development, by regulating the specification of the multipotent stem cell into distinct cell lineages, rather than by differentially regulating differentiation of precommitted precursors. Furthermore, the finding that cell shape can alter stem cell commitment prior to exposure to differentiation factors also provides evidence to support that commitment and differentiation are distinct targets of shape-mediated signaling, and adds to the growing body of evidence that cells can employ the same signaling machinery for different purposes at different stages in their development.

Further examining the role of RhoA, we show that RhoA and Rho kinase (ROCK) activity is greater in spread than unspread cells. Direct manipulation of RhoA signaling replaced the cocktail of differentiation factors present in the media. That is, inactivating RhoA caused adipogenesis while activating RhoA promoted osteogenesis in media containing no differentiation factors. Remarkably, even in osteogenic differentiation media, cells infected with adenovirus encoding dominant-negative RhoA became adipocytes while constitutively active RhoA induced osteogenesis in cells cultured in adipogenic differentiation media. This central role of RhoA in soluble signaling appears quite general, as RhoA has also been shown to regulate IGF-1 mediated adipogenesis and myogenesis (Sordella et al., 2003). The demonstration that cell shape-mediated control of lineage specification also involves RhoA signaling indicates that RhoA may be a ubiquitous integrator of both structural and soluble cues in developmental processes.

Examining the downstream effects of RhoA, we found that the lineage specification signal occurs through the RhoA effector, ROCK, and its effects on myosin-generated cytoskeletal tension. Interestingly, cells expressing dominant-negative RhoA underwent adipogenesis only if cells were round, not spread, while constitutively active RhoA induced osteogenesis only in spread cells. In contrast, constitutive activation of ROCK induced osteogenesis in both round and spread cells, hence bypassing cell shape in regulating stem cell commitment. Thus while RhoA activity can supplant soluble factor signaling, but not cell shape signaling, ROCK is fully downstream of both inductive signals (Figure 8).

The downstream regulation of RhoA signaling by cell shape could occur through multiple mechanisms. Rho GTPase family members require localization to lipid rafts in the plasma membrane to be active (Adamson et al., 1992; Hancock, 2003; Villalba et al., 2001); this localization could be altered by cell shape. Ultimately, the mechanism by which RhoA-ROCK-tension signaling affects stem cell fate may be transduced at focal adhesions.

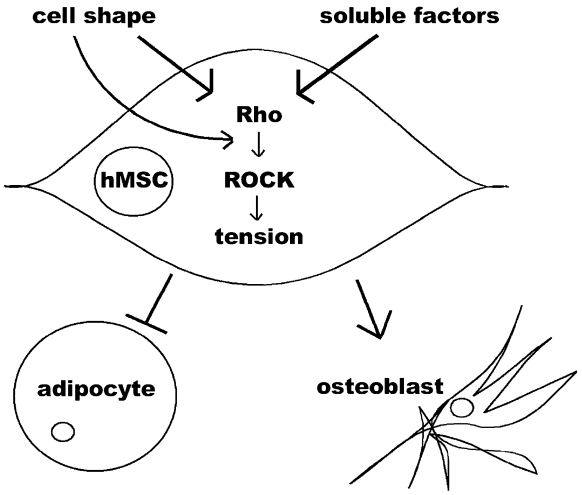

Figure 8. Model of a Mechanically Mediated Switch in hMSC Commitment to Adipogenic or Osteogenic Fate

Cell shape acts as a mechanical cue, driving hMSC commitment between adipocyte and osteoblast when RhoA signaling and cytoskeletal tension are intact. Interference with cell shape, RhoA signaling, ROCK activity, or cytoskeletal tension alters hMSC commitment. RhoA signaling appears necessary and sufficient to replace soluble factor signaling while ROCK activity acts downstream of cell shape.

Changes in cell spreading alter RhoA-mediated cytoskeletal contractility, focal adhesion assembly, and downstream integrin signaling (Riveline et al., 2001; Balaban et al., 2001; Tan et al., 2003; Chen et al., 2003). In all, the interaction between cell shape, biochemical signaling, and cytoskeletal tension demonstrated here highlights the importance of cell structure and mechanics in ultimately determining the mass and nature of connective tissues that develop, and provides a molecular basis for the regulated feedback needed to achieve mechanical homeostasis of these tissues.

It has long been noted that the differentiation of stem cells into multiple lineages is accompanied by dramatic changes in cell morphologies, probably in part due to changes in expression of integrins, cadherins, and cytoskeletal proteins. Here, the demonstration that mechanical cues—as conveyed by changes in cell shape—influence lineage commitment of stem cells not only illustrates the intertwined linkages between cell shape, cytoskeletal mechanics, and developmental processes, but also highlights cell shape itself as a driving factor in development. These linkages likely provide a feedback control mechanism by which complex morphogenetic changes are tied to the programs of tissue specification. While Wolff's law of bone growth and remodeling articulated a century ago that changes in force applied to bone result in changes in its structure, mass, and strength (Wolff, 1892; Vuori, 1996), we have only begun to reveal the intricate molecular connections between tissue structure, function, and mass. Here, investigations into the mechanism of hMSC commitment reveal the importance of these mechanochemical signals, and provide one example of how mechanical cues affect the ever-evolving tissue microenvironment.

Experimental Procedures

Cell Culture and Reagents

Human mesenchymal stem cells were obtained from Cambrex Biosciences and maintained in growth medium, or GM (DMEM, 10% FBS, 0.3 mg/ml glutamine, 100 units/ml penicillin, and 100 μg/ml streptomycin) per Pittenger et al. (2001). Only early passage hMSCs were used for experimental studies. For adipogenic differentiation, hMSCs were exposed to a cycle of 3 days of adipogenic induction medium (GM, 1 μM dexamethasone, 200 μM indomethacin, 10 μg/ml insulin, and 0.5 mM methylisobutylxanthine; Cambrex Biosciences) and then 1 day of adipogenic maintenance medium (GM, 10 μg/ml insulin) chronically. For osteogenic differentiation, hMSCs were cultured in osteogenic differentiation media (GM, 50 μM ascorbic acid-2-phosphate, 10 mM β-glycerophosphate, and 100 nM dexamethasone). Mixed differentiation media (mixed media) contained 1:1 adipogenic induction:osteogenic differentiation media. To inhibit proliferation, cells were exposed to aphidicolin (2 μg/ml; Sigma) chronically or to mitomycin C (10 μg/ml; Sigma) for 2 hr and washed three times with media. Blebbistatin (50 μM; Tocris) was applied with every media change. Cytochalasin D (1 μg/ml; Sigma) and Y-27632 (10 μM; Tocris) were applied daily.

Cell Staining

To stain lipids, cells were fixed in 10% formalin, rinsed in water and then 60% isopropanol, stained with 30 mg/ml Oil red O (Sigma) in 60% isopropanol, and rinsed in water. Alkaline phosphatase was stained using Sigma kit #85 per manufacturer instructions. In brief, samples were fixed in acetone/citrate, rinsed in water, and stained with Fast Blue RR/naphthol. Cells were photographed and counted using a Nikon Eclipse TE200. For total cell counts, nuclei were stained with acridine orange. To assay cell viability, samples were exposed to 4 μM ethidium bromide and 2 μM fluorescein-AM per manufacturer instructions (Molecular Probes), and were counted using a Nikon Eclipse TE200.

FACS Analysis

Cells were stained for alkaline phosphatase using the ELF-97 AP detection kit per manufacturer instructions (Molecular Probes; Telford et al., 2001). In brief, cells were suspended in 0.15 M sodium chloride, filtered through nylon mesh, fixed in 70% ethanol at 4°C for 15 min, washed with 0.15 M sodium chloride and then detection buffer, and exposed to ELF-97 substrate. Cells were analyzed using a He-Cad laser emitting simultaneously at 325 and 488 nm, and fluorescence measured through a 530 nm bandpass filter.

RT-PCR Analysis

Total RNA was isolated using RNA isolation and lipid tissue RNA isolation kits (Qiagen); DNase was removed using RNase-free DNase kit (Qiagen) per manufacturer instructions. 1 μg of total RNA was used in cDNA synthesis with random hexamers as primers (Promega), M-MLV reverse transcriptase, and associated buffers (Invitrogen). Resulting cDNA was used in semiquantitative PCR with established primer sequences (Jaiswal et al., 2000), annealing temperatures of 68°C (PPARγ2), 70°C (β2mg, alkphos), 72°C (Cbfa1), and 84.5°C (Lpl) for 30 cycles.

Fabrication of Micropatterned Substrates

Micropatterned substrates were created per Tan et al. (2002). In brief, PDMS stamps were cast, baked, and removed from master templates, which were previously created using photolithographic methods. Stamps were coated with fibronectin (25 μg/ml; BD) for 2 hr, washed with PBS, and dried with compressed nitrogen. Flat PDMS substrates were UV oxidized for 7 min (UVO-cleaner 342, Jelight Co.), stamped with fibronectin, blocked with Pluronic F108 for 3 hr, and rinsed three times with PBS before cell seeding.

Rho GTPase Assay

RhoA-GTP loading was measured by pull-down assay (adapted from Ren and Schwartz, 2000). Cells were washed with ice-cold TBS, then lysed in 50 mM Tris (pH 7.2) (Quality Biologicals), 1%Triton X-100, 0.5% sodium deoxycholate, 0.1% sodium dodecyl sulfate, 500 mM NaCl, 10 mM $MgCl_2$, 10 μg/ml aprotinin/leupeptin, and 1 mM PMSF (all from Sigma). Lysates were centrifuged 3 min at 3000 rcf at 4°C. Supernatants were incubated with rhotekin binding domain-beads (Upstate) for 45 min at 4°C, centrifuged 3 min at 3000 rcf, washed three times using 50 mM Tris (pH 7.2), 0.5% NP-40, 500 mM NaCl, 1 mM $MgCl_2$, 1 mM EGTA, 10 μg/ml aprotinin/leupeptin, and 1 mM PMSF (all from Sigma), and then suspended in SDS-PAGE buffer (1.5x/1.5% β-mercaptoethanol). RhoA was detected by Western blotting using a monoclonal antibody to RhoA (Santa Cruz Biotechnology). Blots were developed using ECL (Amersham Pharmacia) and quantitated using a digital imager (VersaDoc, Bio-Rad).

ROCK Kinase Assay

Immunoprecipitation was performed as described (Sahai and Marshall, 2002). Cells were lysed in IP buffer (10 mM Tris-HCl at pH 7.5, 1% Triton X-100, 0.5% NP-40, 150 mM NaCl, 2 mM $CaCl_2$, 0.1 mM sodium orthovanadate, 10 μg/ml aprotinin/leupeptin, and 1 mM PMSF [all from Sigma]), then centrifuged at 14,000 rcf for 4 min. Lysate was precleared by incubation with 25 μl Protein G sepharose beads (Amersham Pharmacia) for 15 min and centrifugation for 2 min at 14,000 rcf. Precleared lysate was then incubated with 5 μl of anti-ROCK-II antibody (Santa Cruz Biotechnology) for 30 min, followed by incubation with 50 μl of Protein G sepharose beads. Beads were then washed four times with IP buffer and resuspended in kinase assay buffer (50 mM HEPES [pH 7.4], 150 mM NaCl, 1 mM $MgCl_2$, 1 mM $MnCl_2$, 10 mM NaF, 1 mM sodium orthovanadate, 5% glycerol, 1% NP-40, 1 mM dithiothreitol, and 1 mM PMSF [all from Sigma]). ROCK kinase assay was performed per Ishizaki et al. (2000). ATP (Sigma) and recombinant MYPT1 substrate (Upstate) were incubated with the bead-kinase assay buffer slurry in a reaction volume of 50 μl for 30 min at 37°C, then stopped by SDS-PAGE buffer addition and boiled for 10 min at 95°C. Kinase activity was detected by Western blotting using anti-phospho-MYPT1 (Upstate).

Construction of Recombinant Adenoviruses

RhoA-V14, RhoA-N19, and GFP recombinant adenoviruses were constructed using the AdEasy XL system (Stratagene) according to kit protocols. In brief, cDNA fragments encoding RhoA-V14 and RhoA-N19 were generated via site-directed mutagenesis from WT-RhoA constructs (gifts from M. Philips, New York University and P. Burbelo, Georgetown University), subcloned into pShuttle IRES-GFP1 vectors, then used to transform BJ5813 competent cells containing pADEASY1. Resulting plasmids were linearized and used to transfect HEK293 cells. High titer preparations of resulting adenovirus were obtained by repeated freeze-thaw of cells, cleared by centrifugation, and purified via $CsCl_2$ gradient centrifugation. Viral titer was determined by serial dilution using hMSCs and observing GFP fluorescence after 48 hr. In viral infection experiments, viral MOI resulting in transduction efficiency of at least 80% was added to cells for 4 hr, at which time the media were replaced.

Acknowledgments

This work was supported in part by NIGMS (GM 60692) and NIBIB (EB 00262). R.M. acknowledges support from the NIH Medical Scientist Training Program. D.M.P. was supported in part by the Ruth L. Kirschstein National Research Service Award HL 076060-01. C.M.N. acknowledges support from the Whitaker Foundation. We thank M. Philips and P. Burbelo for the RhoA and GFP constructs, and are grateful to S. Sharkis, A. Saiardi, J. Tan, and D. Gray for helpful discussions.

Received: September 5, 2003
Revised: February 12, 2004
Accepted: February 12, 2004
Published: April 12, 2004

References

Adamson, P., Marshall, C.J., Hall, A., and Tilbrook, P.A. (1992). Post-translational modifications of p21rho proteins. J. Biol. Chem. *267*, 20033–20038.

Balaban, N.Q., Schwartz, U.S., Riveline, D., Goichberg, P., Tzur, G.,

Sabanay, I., Mahalu, D., Safran, S., Bershadsky, A., Addadi, L., and Geiger, B. (2001). Force and focal adhesion assembly: a close relationship studied using elastic micropatterned substrates. Nat. Cell Biol. *3*, 466–472.

Caplan, A.I. (1991). Mesenchymal stem cells. J. Orthop. Res. *9*, 641–650.

Carnac, G., Primig, M., Kitzmann, M., Chafey, P., Tuil, D., Lamb, N., and Fernandez, A. (1998). RhoA GTPase and serum response factor control selectively the expression of MyoD without affecting Myf5 in mouse myoblasts. Mol. Biol. Cell *9*, 1891–1902.

Carvalho, R.S., Schaffer, J.L., and Gerstenfeld, L.C. (1998). Osteoblasts induce osteopontin expression in response to attachment on fibronectin: demonstration of a common role for integrin receptors in the signal transduction processes of cell attachment and mechanical stimulation. J. Cell. Biochem. *70*, 376–390.

Charrasse, S., Meriane, M., Comunale, F., Blangy, A., and Gauthier-Rouviere, C. (2002). N-cadherin-dependent cell-cell contact regulates Rho GTPases and beta-catenin localization in mouse C2C12 myoblasts. J. Cell Biol. *158*, 953–965.

Chen, C.S., Mrksich, M., Huang, S., Whitesides, G.M., and Ingber, D.E. (1997). Geometric control of cell life and death. Science *276*, 1425–1428.

Chen, C.S., Alonso, J.L., Ostuni, E., Whitesides, G.M., and Ingber, D.E. (2003). Cell shape provides global control of focal adhesion assembly. Biochem. Biophys. Res. Commun. *307*, 355–361.

Chrzanowska-Wodnicka, M., and Burridge, K. (1996). Rho-stimulated contractility drives the formation of stress fibers and focal adhesions. J. Cell Biol. *133*, 1403–1415.

Etienne-Manneville, S., and Hall, A. (2002). Rho GTPases in cell biology. Nature *420*, 629–635.

Fajas, L. (2003). Adipogenesis: a cross-talk between cell proliferation and cell differentiation. Ann. Med. *35*, 79–85.

Franceschi, R.T. (1999). The developmental control of osteoblast-specific gene expression: role of specific transcription factors and the extracellular matrix environment. Crit. Rev. Oral Biol. Med. *10*, 40–57.

Friedenstein, A.J. (1976). Precursor cells of mechanocytes. Int. Rev. Cytol. *47*, 327–359.

Green, H. and Kehinde, O. (1974). Sublines of mouse 3T3 cells that accumulate lipid. Cell *1*, 113–116.

Gregoire, F.M., Smas, C.M., and Sul, H.S. (1998). Understanding adipocyte differentiation. Physiol. Rev. *78*, 783–809.

Grigoriadis, A.E., Heersche, J.N., and Aubin, J.E. (1988). Differentiation of muscle, fat, cartilage, and bone from progenitor cells present in a bone-derived clonal cell population: effect of dexamethasone. J. Cell Biol. *106*, 2139–2151.

Gumbiner, B.M. (1996). Cell adhesion: the molecular basis of tissue architecture and morphogenesis. Cell *84*, 345–357.

Hancock, J.F. (2003). Ras proteins: different signals from different locations. Nat. Rev. Mol. Cell Biol. *4*, 373–384.

Hill, C.S., Wynne, J., and Treisman, R. (1995). The Rho family GTPases RhoA, Rac1 and CDC42Hs regulate transcriptional activation by SRF. Cell *81*, 1159–1170.

Hu, E., Tontonoz, P., and Spiegelman, B.M. (1995). Transdifferentiation of myoblasts by the adipogenic transcription factors PPAR gamma and C/EBP alpha. Proc. Natl. Acad. Sci. USA *92*, 9856–9860.

Huang, S., Chen, C.S., and Ingber, D.E. (1998). Control of cyclin D1, p27(Kip1), and cell cycle progression in human capillary endothelial cells by cell shape and cytoskeletal tension. Mol. Biol. Cell *9*, 3179–3193.

Ishizaki, T., Uehata, M., Tamechika, I., Keel, J., Nonomura, K., Maekawa, M., and Narumiya, S. (2000). Pharmacological properties of Y-27632, a specific inhibitor of Rho-Associated Kinases. Mol. Pharmacol. *57*, 976–983.

Jaiswal, R.K., Jaiswal, N., Bruder, S.P., Mbalaviele, G., Marshak, D.R., and Pittenger, M.F. (2000). Adult human mesenchymal stem cell differentiation to the osteogenic or adipogenic lineage is regulated by mitogen-activated protein kinase. J. Biol. Chem. *275*, 9645–9652.

Kimura, K., Ito, M., Amano, M., Chihara, K., Fukata, Y., Nakafuku, M., Yamamori, B., Feng, J., Nakano, T., Okawa, K., et al. (1996). Regulation of myosin phosphatase by Rho and Rho-associated kinase (Rho-kinase). Science *273*, 245–248.

Nelson, C.M., and Chen, C.S. (2002). Cell-cell signaling by direct contact increases cell proliferation via a PI3K-dependent signal. FEBS Lett. *514*, 238–242.

Parfitt, A.M. (1984). Age-related structural changes in trabecular and cortical bone: cellular mechanisms and biomechanical consequences. Calcif. Tissue Int. *36* (*Suppl 1*), S123–S128.

Pavalko, F.M., Chen, N.X., Turner, C.H., Burr, D.B., Atkinson, S., Hsieh, Y.F., Qiu, J., and Duncan, R.L. (1998). Fluid shear-induced mechanical signaling in MC3T3–E1 osteoblasts requires cytoskeleton-integrin interactions. Am. J. Physiol. *275*, C1591–C1601.

Pittenger, M.F., Mackay, A.M., Beck, S.C., Jaiswal, R.K., Douglas, R., Mosca, J.D., Moorman, M.A., Simonetti, D.W., Craig, S., and Marshak, D.R. (1999). Multilineage potential of adult human mesenchymal stem cells. Science *284*, 143–147.

Pittenger, M.F., Flake, A.M., and Deans, R.J. (2002). Stem cell culture: mesenchymal stem cells from bone marrow. In Methods of Tissue Engineering, A. Atala, and R.P. Lanza, eds. (San Diego, CA: Academic Press), pp. 461–469.

Ren, X.D., and Schwartz, M.A. (2000). Determination of GTP loading on Rho. Methods Enzymol. *325*, 264–272.

Ren, X.D., Kiosses, W.B., and Schwartz, M.A. (1999). Regulation of the small GTP-binding protein Rho by cell adhesion and the cytoskeleton. EMBO J. *18*, 578–585.

Riveline, D., Zamir, E., Balaban, N.Q., Schwarz, U.S., Ishizaki, T., Narumiya, S., Kam, Z., Geiger, B., and Bershadsky, A.D. (2001). Focal contacts as mechanosensors: externally applied local mechanical force induces growth of focal contacts by an mDia1-dependent and ROCK-independent mechanism. J. Cell Biol. *153*, 1175–1186.

Rodriguez Fernandez, J.L., and Ben-Ze'ev, A. (1989). Regulation of fibronectin, integrin and cytoskeleton expression in differentiating adipocytes: inhibition by extracellular matrix and polylysine. Differentiation *42*, 65–74.

Roskelley, C.D., Desprez, P.Y., and Bissell, M.J. (1994). Extracellular matrix-dependent tissue-specific gene expression in mammary epithelial cells requires both physical and biochemical transduction. Proc. Natl. Acad. Sci. USA *91*, 12378–12382.

Sahai, E., and Marshall, C.J. (2002). ROCK and Dia have opposing effects on adherens junctions downstream of Rho. Nat. Cell Biol. *4*, 408–415.

Shao, D., and Lazar, M.A. (1997). Peroxisome proliferator activated receptor gamma, CCAAT/enhancer-binding protein alpha, and cell cycle status regulate the commitment to adipocyte differentiation. J. Biol. Chem. *272*, 21473–21478.

Sikavitsas, V.I., Temenoff, J.S., and Mikos, A.G. (2001). Biomaterials and bone mechanotransduction. Biomaterials *22*, 2581–2593.

Smas, C.M., and Sul, H.S. (1997). Molecular mechanisms of adipocyte differentiation and inhibitory action of pref-1. Crit. Rev. Eukaryot. Gene Expr. *7*, 281–298.

Sordella, R., Jiang, W., Chen, G.C., Curto, M., and Settleman, J. (2003). Modulation of Rho GTPase signaling regulates a switch between adipogenesis and myogenesis. Cell *113*, 147–158.

Spiegelman, B.M., and Ginty, C.A. (1983). Fibronectin modulation of cell shape and lipogenic gene expression in 3T3-adipocytes. Cell *35*, 657–666.

Takano, H., Komuro, I., Oka, T., Shiojima, I., Hiroi, Y., Mizuno, T., and Yazaki, Y. (1998). The Rho family G proteins play a critical role in muscle differentiation. Mol. Cell. Biol. *18*, 1580–1589.

Tan, J.L., Tien, J., and Chen, C.S. (2002). Microcontact printing of proteins on mixed self-assembled monolayers. Langmuir *18*, 519–523.

Tan, J.L., Tien, J., Pirone, D.M., Gray, D.S., Bhadriraju, K., and Chen, C.S. (2003). Cells lying on a bed of microneedles: an approach to isolate mechanical force. Proc. Natl. Acad. Sci. USA *100*, 1484–1489.

Telford, W., Cox, W., and Singer, V. (2001). Detection of endogenous

and antibody-conjugated alkaline phosphatase with ELF-97 phosphate in multicolor flow cytometry applications. Cytometry *42*, 117–125.

Thomas, C.H., Collier, J.H., Sfeir, C.S., and Healy, K.E. (2002). Engineering gene expression and protein synthesis by modulating nuclear shape. Proc. Natl. Acad. Sci. USA *99*, 1972–1977.

Thompson, D.W. (1992). On Growth and Form (New York: Dover).

Toma, C.D., Ashkar, S., Gray, M.L., Schaffer, J.L., and Gerstenfeld, L.C. (1997). Signal transduction of mechanical stimuli is dependent on microfilament integrity: identification of osteopontin as a mechanically induced gene in osteoblasts. J. Bone Miner. Res. *12*, 1626–1636.

Villalba, M., Rodriguez, F., Tanaka, Y., Schoenberger, S., and Altman, A. (2001). Vav1/Rac-dependent actin cytoskeleton reorganization is required for lipid raft clustering in T cells. J. Cell Biol. *155*, 331–338.

Vuori, I. (1996). Peak bone mass and physical activity: a short review. Nutr. Rev. *54*, S11–S14.

Watt, F.M., Jordan, P.W., and O'Neill, C.H. (1988). Cell shape controls terminal differentiation of human epidermal keratinocytes. Proc. Natl. Acad. Sci. USA *85*, 5576–5580.

Wei, L., Zhou, W., Croissant, J.D., Johansen, F.E., Prywes, R., Balasubramanyam, A., and Schwartz, R.J. (1998). RhoA signaling via serum response factor plays an obligatory role in myogenic differentiation. J. Biol. Chem. *273*, 30287–30294.

Welsh, C.F., Roovers, K., Villanueva, J., Liu, Y., Schwartz, M.A., and Assoian, R.K. (2001). Timing of cyclin D1 expression within G1 phase is controlled by Rho. Nat. Cell Biol. *3*, 950–957.

Wolff, J. (1892). Das gasetz der transformation der knochen. (Berlin).